Comparison of the new wind flow model FUROW with WAsP and OpenFOAM for different topographic features

Javier Magdalena*, Héctor Burgueño, Elliott Baché, Alberto Tejón, Aureliano Robles

SOLUTE Ingenieros, Madrid, Spain

Abstract

SOLUTE has developed a new software for wind data analysis, wind resource assessment, energy production estimation and class verification called FUROW. This software has its own wind flow model which allows calculating wind speed and turbulence at multiple heights based on wind measurements and taking into account topographic effects (orography and roughness) as well as thermal stability of the site.

The FUROW model has been compared with WAsP and OpenFOAM models in order to characterize its behavior under different orographic and roughness conditions. For this purpose, wind speed has been simulated over Gaussian hills with changing average slopes, and modified roughness in order to simulate different land cover types. The wind speed vertical profiles have initially been calibrated on flat terrain, adjusting the Monin-Obukhov length in FUROW to approximate as closely as possible the WAsP profile in each case. Three wind speed values have been run in order to cover the typical range of observed wind speed distributions. Simulation results have been compared at different reference points along a horizontal transect evaluating the difference in the vertical profile obtained by the three models. Conclusions derived from this study indicate that FUROW produces comparable results to those obtained by WAsP and OpenFOAM along the Gaussian hill. Although more comparisons over non ideal orographies should be performed including comparison with on site measurements, it has been proved that the overestimation in FUROW of wind speed in very complex terrain is less pronounced than in WAsP when compared with a CFD solution.

Keywords:
FUROW, WAsP, OpenFOAM, Wind profile, Atmospheric stability

1. Introduction

Since the late 1980s many wind flow models have been developed in order to accurately predict the wind resource at a given area where wind farms are going to be installed. The first wind farms were installed in areas characterized by smooth orography, that is, hills with gentle slopes to ensure attached flows such us those found in Northern Europe. The models that were developed to simulate these locations were linear flow models [1, 2], such as Wind Atlas Analysis and Application Program (WAsP) [3], that were sufficient for the simple terrain. As the sector has grown and expanded worldwide, sites with more complex terrain and special atmospheric stratification features have appeared. Although these characteristics are not within the application envelope of linear models, the latter are still being used to perform wind resource assessment, due to a reasonable accuracy at low computational costs. Nevertheless, large discrepancies may impact the predicted energy production exceedance values.

In response to these discrepancies, CFD models, such as OpenFOAM, and commercial software, such as WindSim and Meteodyn, were developed in order to improve wind resource estimations over complex terrain or even under peculiar atmospheric stability conditions. These models solve the Reynolds-averaged Navier-Stokes equations assuming an incompressible and steady state flow, using different turbulence models, among them the well-known k-ϵ model. Due to the larger number of equations to be solved and the smaller grid resolution necessary to accurately resolve the equations, much higher computational times than the linear flow models are required. On the other hand, they handle flow separation and turbulence much better than linear models, allowing steep hills and uneven terrain to be handled more accurately.

There exists more sophisticated types of model, which couple microscale models with mesoscale data [4]. These models are composed of a numerical weather prediction (NWP) model, such as weather research and forecasting (WRF) model that simulates on scales of about $10km$ coupled with a CFD solver, such as OpenFOAM, which resolves on much smaller scales. These models are typically more precise than the linear models and the standalone CFD models since they model the radiation, humidity, cloud processes, condensation, rain, and other atmo-

*Corresponding author: javier.magdalena@solute.es

spheric conditions, in addition to the turbulence and viscous forces modeled in the CFD sub-grid. The models have become an important tool in order to improve wind resource estimations and reduce errors, but they require significantly more computational time and development.

In this paper we show the behavior of a new linear wind flow solver implemented in FUROW, and the sensitivity to different orographical input data when it is compared with WAsP. The model is then verified with OpenFOAM, which should provide a better approximation to reality. Velocity profiles, speed-ups, and wind shear are compared between the different models. These values are studied for different inlet velocities and hill slopes; it is critical to study the effects of the slope of a hill as linear models tend to overestimate wind speed in complex terrain and need further corrections to improve estimations as proposed in [5].

2. Description of wind flow models

2.1. WAsP model

WAsP is perhaps the most common software used in the wind industry to estimate wind resources. The WAsP orographic model is based on conclusions of the Jackson and Hunt theory [1] on which flow perturbations created by hills are represented by a modified potential flow. All of these models are based on the linearization of the equations of motion in cartesian coordinates for neutral flow perturbations relative to a reference wind speed; however, the WAsP model is somewhat different as it uses polar zooming grid with the finest resolution centered on the point of interest. The whole method and the equations are described in [2].

The calculation logic of WAsP model is as follows and is represented in Figure 1:

1. Wind and direction measurements are represented by the Observed Wind Climate (OWC) to obtain the site statistics and fitted Weibull distributions.
2. The OWC together with local site topographic conditions create the local wind, which is cleaned from local disturbances in order to obtain a Generalized Wind Climate for several standard conditions via geostrophic wind.
3. The Generalized Wind Climate plus the terrain description are applied to any calculation point adding local disturbances to calculate the Predicted Wind Climate (PWC).

Formulations for linear models such as WAsP are based on neutral conditions on which the logarithmic profile is used for wind profile description on the surface layer. However, when atmospheric conditions are not neutral, vertical profiles need a more generic expression that depends upon a stability parameter, which is usually the so-called Monin-Obukhov length.

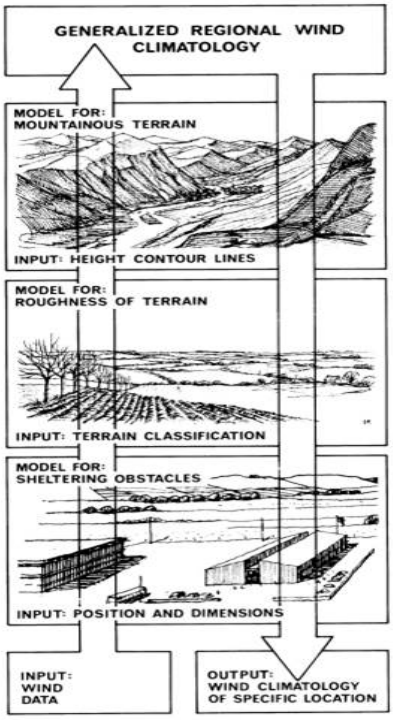

Figure 1: WAsP wind atlas methodology

As described in [6], the WAsP model considers a height of minimum response to stability effects, where it is possible to calculate the deviations relative to neutral conditions. These deviations account for changes in friction velocity and the wind profile due to atmospheric stability effects. Both effects are modeled in WAsP by changing the average surface heat flux and its variability ($\Delta H_{off}, \Delta H_{rms}$). As per [7], the wind profile is more sensitive to the first parameter than to the second one. The representative values for onshore conditions of these two parameters for Europe are ($\Delta H_{off} = -40 W/m^2$; $\Delta H_{rms} = 100 W/m^2$) although the selection of these parameters should be modified for each site to match with local atmospheric conditions. For ΔH_{off}, negative values indicate more stable conditions, values close to 0 refer to neutral conditions, and positive values provide unstable conditions. Typical values of ΔH_{off} and ΔH_{rms} for offshore conditions are $-8 W/m^2$ and $30 W/m^2$.

2.2. FUROW model

The physical model used by FUROW in wind speed calculations is based on the UPMORO code first developed by the Research Group “Mecánica de Fluidos aplicada a la Ingeniería Industrial” belonging to the Universidad Politécnica de Madrid - Escuela Técnica Superior de Ingenieros Industriales (UPM-ETSII) (see [8] and [9]). FUROW has been improved and optimized from the original UPMORO code.

The FUROW model estimates the effect of orography and roughness on wind speed and wind direction at a particular point and height by calculating the geostrophic wind and assuming its invariance for the whole map. This hypothesis is ensured if wind measurements are centered on the area where wind calculations are performed and the calculation area is not very large (several kilometers as a radius from map center, *i.e.* 4km).

To consider the orography, UPMORO was based on one of the flow potential linearized models. Again, this model is applicable to configurations with gentle slopes (in general less than 16^o or 30%), while for steeper areas errors could be higher as in other linearized wind flow models such as WAsP model or MS-Micro. UPMORO model is based on the theory proposed by Jackson and Hunt on [1], and later revised by Belcher and Hunt on [10]. This theory establishes that the wind flow field is divided in three different layers, each one being characterized by different acceleration factors which take into account the effect of the slope around the calculation point as well as the roughness length:

- Upper layer: this region is characterized by irrotational flow (thus deriving from a potential function) and ideal.
- Middle layer: this region is characterized by rotational flow with turbulent stresses.
- Inner layer: this region is mainly affected by friction and wind speed decreases to 0 at the surface.

The calculation logic of FUROW model is as shown in Figure 2 and summarized below:

1. Wind and direction measurement statistics summarized on a so-called Clima Object are “cleaned” from disturbances such as orography and roughness, thus providing a wind speed and direction as if they had been measured on “flat terrain”. Atmospheric stability effects are also taken into account.
2. “Flat terrain” wind speed and direction are modified via a geostrophic drag law to derive the geostrophic wind, which is assumed to be invariant around the site.
3. Wind speed and direction can be calculated at any point by adding the effects of orography and roughness around the point, as well as the particular effects of atmospheric stability included in the Clima Object.

In regards to the vertical wind profile, the formulation in FUROW is based on the proposed wind profiles described in [11]. Geostrophic wind is calculated through the formulation proposed by Garrat in [12] as follows:

$$G = \frac{u_*}{\kappa}\sqrt{\left(\ln\left(\frac{h_{PBL}}{z_0}\right) - A(\mu)\right)^2 + B(\mu)^2} \tag{1}$$

where u_* is the friction velocity, $\kappa = 0.41$ is the Von Karman constant, z_0 is the characteristic atmospheric roughness length, A(μ) and B(μ) are functions that depend upon the atmospheric stability, and h_{PBL} is the planetary boundary layer height, which is proportional to the ratio between friction velocity and the Coriolis parameter. The shape of the wind profile is determined by different parameters such as roughness length, atmospheric stability and geostrophic wind. Depending on the atmospheric stability conditions, wind profiles adopt different formulations.

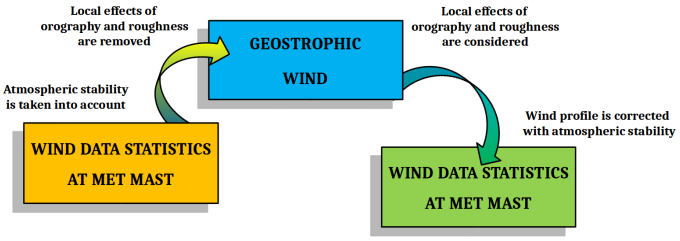

Figure 2: FUROW calculation procedure

a. Neutral conditions

$$U(z) = \frac{u_*}{\kappa}\left[ln\left(\frac{z}{z_0}\right) + \frac{z}{L_{MBL}} - \frac{z}{h_{PBL}}\left(\frac{z}{2L_{MBL}}\right)\right] \tag{2}$$

b. Stable conditions

$$U(z) = \frac{u_*}{\kappa}\left[ln\left(\frac{z}{z_0}\right) + \phi_s\left(\frac{z}{L}\right)\left(1 - \frac{z}{2h_{PBL}}\right) + \frac{z}{L_{MBL}} + -\frac{z}{h_{PBL}}\left(\frac{z}{2L_{MBL}}\right)\right] \tag{3}$$

c. Unstable conditions

$$U(z) = \frac{u_*}{\kappa}\left[\ln\left(\frac{z}{z_0}\right) + \phi_u\left(\frac{z}{L}\right) + \frac{z}{L_{MBL}} - \frac{z}{h_{PBL}}\left(\frac{z}{2L_{MBL}}\right)\right] \tag{4}$$

where U is the velocity parallel to sea level or any other fixed altitude, z is the height, L_{MBL} is a length scale related to the middle part of the boundary layer, and the stability functions ϕ_s and ϕ_u are defined in Eqs. (5) and (6) and depend on the stability parameter which is defined as z/L, being L the Monin-Obukhov length.

$$\phi_s\left(\frac{z}{L}\right) = b\frac{z}{L} \tag{5}$$

$$\phi_u\left(\frac{z}{L}\right) = \frac{3}{2}\ln\left(\frac{1+x+x^2}{3}\right) - \sqrt{3}\arctan\left(\frac{1+2x}{\sqrt{3}}\right) + \frac{\pi}{\sqrt{3}}$$
$$x = \left(1 - 12\frac{z}{L}\right)^{-1/3} \tag{6}$$

where the coefficient *b* has been found to be close to 5 as indicated in [13] and it is well reported in literature and experiments regarding Monin-Obukhov Similarity

Theory (MOST). However, under very stable conditions, *i.e.*, when z/L is approximately greater than 1 or 2, Yagüe et al. remark in [14] that the similarity function differs from MOST predictions as the similarity function tends to level off. Since the late 1950s, experimental data suggest values of $b = 2$ for very stable conditions, although this value has a wide spread. For this reason, the coefficient *b* has been parametrized in FUROW as a function of Monin-Obukhov length itself. Depending on the atmospheric stability this proportionality is different, in such a way that under stable conditions, boundary layer height is lower than under unstable or neutral conditions.

To describe the wind profile below forest height, the most commonly used expression is the one proposed on [15], which has an exponential form. The formula has been modified including the forest porosity such that vertical profile is described as:

$$U(z) = U(h)\exp\left(-\alpha_v(1-P)\frac{h-z}{h}\right) \tag{7}$$

where α_v is a constant depending on the vegetation type and leafiness, h is the canopy height (which is proportional to the roughness length) and *P* is the forest porosity such that for normal forest density a value of 0.45 is considered.

More information about the formulation used in the FUROW model and other modules of the software are described in [16].

2.3. OpenFOAM model

The results obtained via FUROW and WAsP are compared with the results from a more representative model created in OpenFOAM [17]. This model solves a system of non-linear partial differential equations for the entire 3D domain, discretizing the orography and assuming a uniform characteristic roughness length. The wind profiles (as calculated in §2.2) are imposed as boundary conditions of the domain. The wind profiles throughout the domain are then calculated using the OpenFOAM environment, and FUROW and WAsP are subsequently compared to the results. In the OpenFOAM simulations presented in this article, the Reynolds-averaged Navier-Stokes equations for steady-state, incompressible, turbulent flow are modeled [18] as follows:

$$\begin{aligned}
&\frac{\partial U_i}{\partial x_i} = 0 \qquad i = 1,2,3\\
&\rho\frac{\partial}{\partial x_j}(U_iU_j) = -\frac{\partial p}{\partial x_i} + \frac{\partial}{\partial x_j}(2\mu S_{ij} - \rho\overline{u_i'u_j'}) \qquad i,j = 1,2,3,
\end{aligned} \tag{8}$$

where *i* and *j* are the tensor indices following standard tensor notation, $\frac{\partial}{\partial x_i}$ represents the gradient vector, ρ is the density, *p* is the pressure, μ is the dynamic viscosity, u' is the fluctuating component of the velocity, and S_{ij} is the mean strain-rate tensor defined by

$$S_{ij} = \frac{1}{2}\left(\frac{\partial U_i}{\partial x_j} + \frac{\partial U_j}{\partial x_i}\right) \qquad i = 1,2,3. \tag{9}$$

Although many turbulunce closure models are available, typically the $k-\epsilon$ model is used for flow over complex terrains. This closure model is a semi-empirical model that assumes fully turbulent flow and solves equations for the turbulent kinetic energy k and its dissipation rate ϵ. The equations are as follows:

$$\begin{aligned}
&\nu_T = C_\mu k^2/\epsilon\\
&\frac{\partial k}{\partial t} + U_j\frac{\partial k}{\partial x_j} = \tau_{ij}\frac{\partial U_i}{\partial x_j} - \epsilon + \frac{\partial}{\partial x_j}\left[(\nu + \nu_T/\sigma_k)\frac{\partial k}{\partial x_j}\right]\\
&\frac{\partial \epsilon}{\partial t} + U_j\frac{\partial \epsilon}{\partial x_j} = C_{\epsilon 1}\frac{\epsilon}{k}\tau_{ij}\frac{\partial U_i}{\partial x_j} - C_{\epsilon 2}\frac{\epsilon^2}{k} + \frac{\partial}{\partial x_j}\left[(\nu + \nu_T/\sigma_\epsilon)\frac{\epsilon}{\partial x_j}\right]
\end{aligned} \tag{10}$$

having chosen the following constant values as in [19] $C_{\epsilon 1} = 1.44$, $C_{\epsilon 2} = 1.92$, $C_\mu = 0.09$, $\sigma_k = 1.0$, and $\sigma_\epsilon = 1.3$.

A hexahedral, structured mesh of approximately two million elements is used, with a mesh refinement near the terrain. To avoid excessive boundary layer elements, a wall function is employed to compute the velocity near the wall.

$$\frac{u_p}{u*} = \frac{1}{\kappa}ln\left(\frac{Ez_p}{C_sk_s}\right) \tag{11}$$

where u_p is the velocity near the wall (at the cell centroid), $E \approx 9.793$, z_p is the distance from the wall to the nearest cell centroid, $C_s = 0.327$, $u* = C_\mu^{0.25}k^{0.5}$, and $k_s = 20z_0$.

The 3D domain is defined as a rectangular prism with the following faces: x_-, x_+, y_-, y_+, z_-, z_+. The prism is defined with the Gaussian hill rising in the z-direction and the flow in the positive x-direction (entering through the plane x_-. The boundary conditions may be seen in Table 1, where $\partial/\partial n$ is the partial derivatie with respect to the normal direction, $\mathbf{U}_n$ is the normal velocity, and $\mathbf{U}_t$ is the tangential velocity. Initially, the inlet wind profile is applied throughout the domain. The pressure is initialized to zero everywhere.

Plane	Velocity	Pressure
x_-	$\mathbf{U}_n = f(z)\mathbf{n}$	$\partial p/\partial n = 0$
x_+	$\partial\mathbf{U}/\partial n = \mathbf{0}$	$p = 0$
y_-	$\mathbf{U}_n = \mathbf{0}$ & $\partial\mathbf{U}_t/\partial n = \mathbf{0}$	$\partial p/\partial n = 0$
y_+	$\mathbf{U}_n = \mathbf{0}$ & $\partial\mathbf{U}_t/\partial n = \mathbf{0}$	$\partial p/\partial n = 0$
z_-	$\mathbf{U} = \mathbf{0}$	$\partial p/\partial n = 0$
z_+	$\mathbf{U}_n = \mathbf{0}$ & $\partial\mathbf{U}_t/\partial n = \mathbf{0}$	$\partial p/\partial n = 0$

Table 1: OpenFOAM model boundary conditions

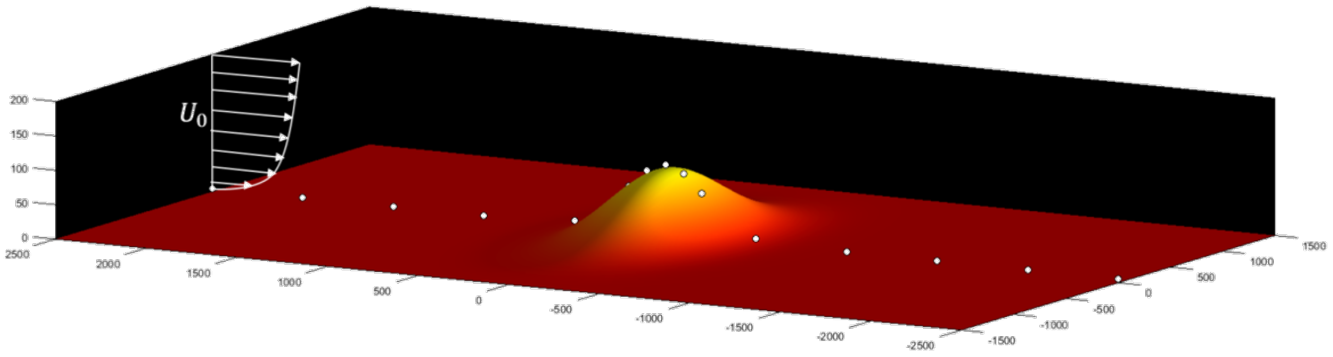

Figure 3: Experiment set-up for a 20% slope Gaussian hill

3. Experiments and results

This section presents the experimental part of the study. First, the input data used for all simulations is presented. Second, the calibration between both models is described. Finally, the results for different configurations in terms of wind speed and vertical wind shear are shown.

3.1. Data used for the study

In order to perform the comparison between both models, a set of Gaussian shaped hills with different average slopes ranging from 10% up to 50% have been used. The characteristic dimensions of the Gaussian hills are described in Table 2.

Various land cover types are modeled with three different roughness lengths: 0.03 (typical of smooth terrain with natural grassland and pastures), 0.10 (typical of crops, bushes and fruit trees) and 0.40 (typical of agro-forestry areas, construction sites and low forest areas).

Finally, wind speed reference values have been simulated at a low wind speed (LWS) of 5m/s, medium wind speed (MWS) of 10m/s and high wind speed (HWS) of 15m/s in order to cover the typical range of observed wind speed distributions. The reference height has been set to 80m as most of current meteorological masts are of this height. The wind input position is located on flat terrain and 2500m away from the hilltop. Wind direction has been chosen to be from the west (270°). The wind profile used for every wind speed class and roughness has been defined as explained in the following section.

An example of a Gaussian hill for an average slope of 20% and the complete set-up for obtaining the calculated data is shown in Fig. 3.

3.2. Calibration of models

In order to compare the FUROW and WAsP models, a calibration is performed to ensure the same experimental conditions. The two models are used to simulate a flat terrain with varying roughness lengths. For this purpose the atmospheric stability parameter in FUROW, which is the Monin-Obukhov length, has been modified iteratively in order to minimize the root mean square deviation (RMSD) between the vertical profile simulated in FUROW and that derived from WAsP for the program default conditions ($\Delta H_{off} = -40W/m^2$; $\Delta H_{rms} = 100W/m^2$), which are considered to be slightly stable conditions and representative for Europe.

Average slope (%)	Hill height (m)	Long axis (m)	Short axis (m)
10	100	500	500
20	100	500	250
30	100	500	167
40	100	500	125
50	100	500	100

Table 2: Gaussian hill parameters.

Roughness length (m) / Wind speed class	LWS 5m/s	MWS 10m/s	HWS 15m/s
z_0=0.03	50	170	700
z_0=0.1	65	350	1500
z_0=0.4	150	10000	10000

Table 3: Selected Monin-Obukhov length

Roughness length (m) / Wind speed class	LWS 5m/s	MWS 10m/s	HWS 15m/s
z_0=0.03	0.55%	0.10%	0.10%
z_0=0.10	0.25%	0.18%	0.14%
z_0=0.40	0.98%	0.78%	0.93%

Table 4: RMSD of speed-up for FUROW & WAsP between 30m and 130m

Simulation	WAsP			FUROW		
	$\alpha(30-50m)$	$\alpha(50-90m)$	$\alpha(90-130m)$	$\alpha(30-50m)$	$\alpha(50-90m)$	$\alpha(90-130m)$
LWS z_0=0.03	0.202	0.247	0.279	0.214	0.234	0.251
LWS z_0=0.10	0.228	0.255	0.284	0.240	0.255	0.270
LWS z_0=0.40	0.266	0.281	0.302	0.322	0.263	0.268
MWS z_0=0.03	0.161	0.168	0.178	0.164	0.167	0.174
MWS z_0=0.10	0.183	0.179	0.183	0.184	0.178	0.178
MWS z_0=0.40	0.227	0.210	0.202	0.271	0.200	0.185
HWS z_0=0.03	0.145	0.139	0.137	0.146	0.139	0.136
HWS z_0=0.10	0.172	0.160	0.154	0.184	0.160	0.152
HWS z_0=0.40	0.221	0.199	0.185	0.270	0.198	0.183

Table 5: Vertical wind shear values for flat terrain

In this section, the RMSD has been calculated with a range of heights between 30m and 130m. Heights smaller than 30m are omitted for the RMSD calculation since the two models differ significantly for large roughness lengths and low heights due to different treatment of the canopy layer. The definition to calculate the RMSD for calibrating FUROW with WAsP is thus:

$$RMSD_{fw} = \sqrt{\frac{1}{6}\sum_{i=1}^{i=6}\left(\frac{v_{i,f}-v_{i,w}}{v_{i,w}}\right)^2} \quad (12)$$

where $v_{i,f}$ represents the wind speed at height *i* modeled with FUROW, and $v_{i,w}$ is the wind speed at height *i* modeled with WAsP. Selected Monin-Obukhov lengths and RMSD values are shown in Table 3 and Table 4. As can be noted from the data in Table 4, the profiles for high roughness lengths compare less well. The different treatment of the canopy layer is evident here.

The wind shear should also be similar between the two models since it is derived from the velocity profiles that were matched minimizing root mean square deviations. Trends between the two models for vertical wind shear are described below:

- Simulated wind shear is in most cases similar for FUROW and WAsP. On average, predicted wind shear by FUROW at lower levels is slightly above that predicted by WAsP, is similar for medium heights, and is slightly lower for higher levels.
- Near the terrain, the largest differences may be found due to the different models used to model wind profiles within the roughness length. FUROW predicts a higher wind shear close to the surface for larger roughness lengths.
- Wind shear decreases as wind speed increases for a constant roughness length, and wind shear increases as roughness length increases.
- For low wind speeds, wind shear tends to increase with height, whereas for medium and high wind speeds shear remains constant or decreases for both models.

Atmospheric Stability	Monin-Obukhov length range
Very unstable	-50 < L < 0
Unstable	-200 < L < -50
Slightly unstable	-1000 < L < -200
Neutral	$\|L\|$ >1000
Slightly stable	1000 > L > 200
Stable	200 > L > 50
Very stable	50 > L >0

Table 6: Atmospheric stability classification

According to the Monin-Obukhov calculations (see Table 3), the profiles for medium wind speeds and high wind speeds can be classified as slightly stable or neutral (see Table 6 for atmospheric stability classification), whereas for low wind speeds, stable conditions are more prominent. Based on these figures, it could be stated that in order to reproduce slightly stable conditions for low wind speeds, the parameter ΔH_{off} should be even more negative.

3.3. Results at hilltop

In this subsection, results at the hilltop are presented, as this would be the preferable site to place a wind turbine on a wind farm. The initial wind profile generated for each variation of wind speed and roughness is given by the Monin-Obukhov length, determined in the calibration stage.

3.3.1. Slope and roughness changes

The effect of the slope in terms of the increase in initial wind speed has been calculated at the hilltop position for all slopes and different roughness length values. The results for a representative case with MWS conditions, roughness length of 0.10m and 5 different slopes (from 10% up to 50%) are presented in Fig. 4, and the results for two different heights are presented in Fig. 5. Results for speed-up difference between FUROW and WAsP

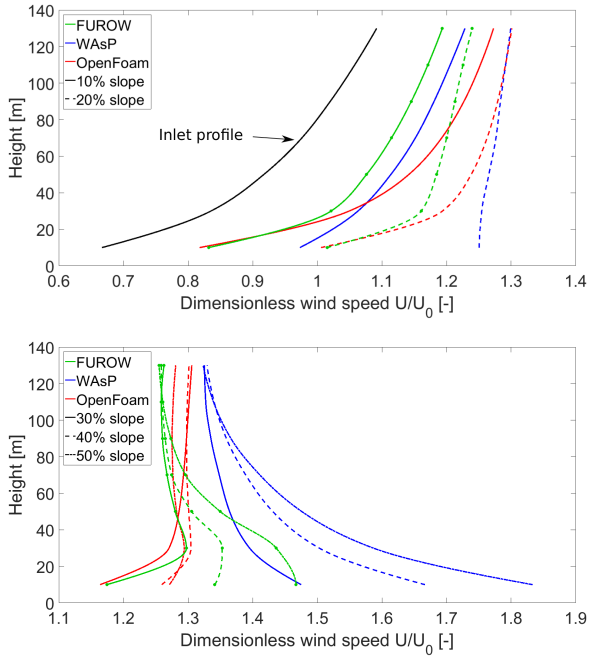

Figure 4: Wind speed profiles at hilltop for MWS and $z_0 = 0.10$

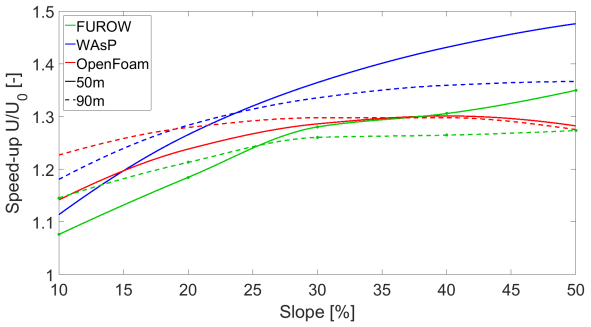

Figure 5: Wind speed-up at hilltop for MWS, $z_0 = 0.10$, and 50m or 90m

($D_{i,fw}$) for a roughness length of 0.10m are also presented in Table 7. The speed-up difference between FUROW and WAsP is calculated as follows:

$$D_{i,fw} = \frac{v_{i,f}}{v_{ref,f}} - \frac{v_{i,w}}{v_{ref,w}}, \tag{13}$$

where $v_{ref,f}$ and $v_{ref,w}$ are the reference speeds at 80m for FUROW and WAsP respectively. Only this roughness length is reported since the trends remain the same as for the other roughness lengths. The only difference between results for different roughness lengths is the expected dissimilarity between FUROW and WAsP for high roughness lengths and low heights.

Results for speed-up difference between FUROW and OpenFOAM at height *i* ($D_{i,fo}$) and between WAsP and OpenFOAM at height *i* ($D_{i,wo}$) are also presented in Table 8. The speed-up difference between FUROW and OpenFOAM or WAsP and OpenFOAM is calculated as

		Slope (%)				
	Height (m)	10.00	20.00	30.00	40.00	50.00
LWS	10	-0.14	-0.23	-0.30	-0.33	-0.37
	30	-0.05	-0.11	-0.12	-0.19	-0.25
	50	-0.05	-0.10	-0.11	-0.16	-0.21
	70	-0.05	-0.10	-0.11	-0.15	-0.19
	90	-0.05	-0.09	-0.10	-0.13	-0.15
	110	-0.05	-0.09	-0.10	-0.11	-0.13
	130	-0.05	-0.09	-0.10	-0.11	-0.12
	Profile (30-130)	-0.05	-0.10	-0.11	-0.14	-0.18
MWS	10	-0.14	-0.24	-0.30	-0.33	-0.37
	30	-0.04	-0.09	-0.10	-0.16	-0.23
	50	-0.04	-0.08	-0.08	-0.13	-0.18
	70	-0.04	-0.08	-0.08	-0.12	-0.16
	90	-0.04	-0.07	-0.07	-0.10	-0.12
	110	-0.03	-0.07	-0.07	-0.08	-0.10
	130	-0.04	-0.06	-0.06	-0.07	-0.09
	Profile (30-130)	-0.04	-0.07	-0.08	-0.11	-0.15
HWS	10	-0.14	-0.24	-0.31	-0.33	-0.37
	30	-0.04	-0.09	-0.09	-0.16	-0.23
	50	-0.04	-0.08	-0.08	-0.13	-0.18
	70	-0.03	-0.07	-0.07	-0.12	-0.15
	90	-0.03	-0.07	-0.07	-0.09	-0.12
	110	-0.03	-0.06	-0.06	-0.08	-0.10
	130	-0.03	-0.05	-0.05	-0.07	-0.08
	Profile (30-130)	-0.03	-0.07	-0.07	-0.11	-0.14

Table 7: Hilltop speed-up difference for FUROW vs. WAsP with z_0 = 0.1m (red values correspond to larger deviations while green values correspond to smaller deviations).

follows:

$$D_{i,fo} = \frac{v_{i,f}}{v_{ref,f}} - \frac{v_{i,o}}{v_{ref,o}}$$
$$D_{i,wo} = \frac{v_{i,w}}{v_{ref,w}} - \frac{v_{i,o}}{v_{ref,o}} \tag{14}$$

where $v_{i,o}$ is the OpenFOAM velocity at height *i*, and $v_{ref,o}$ is the reference velocity at 80m for OpenFOAM. The following conclusions can be extracted from the results:

- FUROW wind speed predictions are lower than those obtained by WAsP, with larger differences between FUROW and WAsP as the average hill slope increases. In most cases except for very large slopes, FUROW wind speed predictions are lower than those obtained by OpenFOAM.
- Lower wind speeds yield higher relative differences between both models than medium or high wind speeds. They also yield higher differences between FUROW and OpenFOAM.
- Wind speed difference between models decreases as height increases.
- For complex terrain (slopes above 30%), linearized models produce higher accelerations close to the ground than those predicted by OpenFOAM, being especially pronounced in WAsP. FUROW shows similar behavior to OpenFoam in middle layers but slightly underestimates wind speed at higher levels, whereas WAsP overestimates at any height.
- Roughness length does not cause major differences between models in the wind speed-up, except for the smaller heights ($\leq 30m$), as FUROW is more sensitive

to the roughness length and gives speed-ups that are much closer to those given by OpenFOAM.

		Furow					WAsP				
		Slope (%)					Slope (%)				
	Height (m)	10.00	20.00	30.00	40.00	50.00	10.00	20.00	30.00	40.00	50.00
LWS	10	-0.271	-0.321	-0.307	-0.220	0.027	-0.130	-0.087	-0.008	0.108	0.395
	30	-0.237	-0.232	-0.181	-0.169	-0.102	-0.183	-0.121	-0.057	0.017	0.151
	50	-0.210	-0.200	-0.163	-0.160	-0.116	-0.162	-0.104	-0.053	-0.001	0.091
	70	-0.180	-0.171	-0.142	-0.145	-0.120	-0.127	-0.070	-0.030	0.007	0.068
	90	-0.152	-0.143	-0.122	-0.121	-0.110	-0.105	-0.051	-0.019	0.007	0.044
	110	-0.126	-0.118	-0.101	-0.099	-0.098	-0.077	-0.028	-0.003	0.013	0.033
	130	-0.103	-0.092	-0.078	-0.079	-0.087	-0.049	-0.004	0.017	0.027	0.031
	Profile	-0.183	-0.183	-0.156	-0.142	-0.087	-0.119	-0.066	-0.022	0.025	0.116
MWS	10	0.014	0.009	0.009	0.082	0.196	0.155	0.245	0.310	0.407	0.562
	30	-0.028	-0.033	0.025	0.037	0.065	0.014	0.061	0.123	0.199	0.293
	50	-0.065	-0.054	-0.007	-0.004	0.011	-0.028	0.027	0.077	0.130	0.194
	70	-0.078	-0.063	-0.027	-0.030	-0.022	-0.041	0.014	0.054	0.091	0.135
	90	-0.081	-0.066	-0.039	-0.038	-0.033	-0.046	0.004	0.036	0.062	0.091
	110	-0.081	-0.066	-0.045	-0.043	-0.040	-0.047	0.000	0.024	0.042	0.062
	130	-0.079	-0.061	-0.045	-0.046	-0.044	-0.044	-0.002	0.018	0.028	0.043
	Profile	-0.057	-0.048	-0.018	-0.006	0.019	-0.005	0.050	0.092	0.137	0.197
HWS	10	-0.120	-0.160	-0.139	-0.025	0.281	0.024	0.079	0.166	0.305	0.653
	30	-0.115	-0.096	-0.036	-0.010	0.143	-0.074	-0.003	0.058	0.149	0.369
	50	-0.095	-0.082	-0.039	-0.027	0.074	-0.059	-0.004	0.041	0.104	0.253
	70	-0.080	-0.072	-0.040	-0.038	0.032	-0.046	0.000	0.034	0.077	0.182
	90	-0.069	-0.064	-0.039	-0.035	0.013	-0.037	0.001	0.029	0.058	0.132
	110	-0.060	-0.056	-0.037	-0.033	0.001	-0.029	0.004	0.025	0.044	0.097
	130	-0.053	-0.047	-0.032	-0.032	-0.008	-0.023	0.006	0.022	0.034	0.072
	Profile	-0.084	-0.082	-0.052	-0.029	0.077	-0.035	0.012	0.054	0.110	0.251

Table 8: Hilltop speed-up difference for FUROW vs. OpenFOAM & WAsP vs. OpenFOAM with z_0 = 0.1m (green values correspond to positive deviations & blue values correspond to negative deviations).

3.3.2. Vertical wind shear

Vertical wind shear has been calculated on two different levels in order to compare the performance of each model. An appropriate determination of the wind shear has a remarkable influence on vertical extrapolations when measurement mast height is relatively low.

Wind shear has been calculated based on the following definition:

$$\alpha = \frac{\ln\left(\frac{V_2}{V_1}\right)}{\ln\left(\frac{Z_2}{Z_1}\right)} \tag{15}$$

where V_2 and V_1 are the wind speeds at the top and the bottom of the interval and Z_2 and Z_1 the respective heights. The differences in the results for different slopes are coherent with the results reported in §3.2 for a flat terrain. Results in Table 9 (positive values indicate a higher wind shear for FUROW) show the similarities and differences, predicting the same trends between both models. The results are only presented for a roughness length of 0.1m since the trends are the same for all roughness lengths. Wind shear differences of FUROW and WAsP with OpenFOAM may be seen in Table 10. The simulations reveal that the wind shear results from this comparison agree less than between FUROW and WAsP. This, of course, is to be expected since both are based on linear models while OpenFOAM solves the non-linearity. Some of the trends and important remarks found for the comparisons between FUROW and OpenFOAM and between WAsP and OpenFOAM are:

		Slope (%)				
	Alpha	10.00	20.00	30.00	40.00	50.00
LWS	10-50	0.078	0.089	0.100	0.077	0.081
	50-90	0.008	0.014	0.013	0.037	0.038
	90-130	-0.008	0.021	0.023	0.047	0.051
MWS	10-50	0.076	0.088	0.102	0.078	0.083
	50-90	0.007	0.017	0.010	0.033	0.032
	90-130	0.004	0.026	0.026	0.047	0.048
HWS	10-50	0.077	0.090	0.103	0.079	0.085
	50-90	0.008	0.018	0.012	0.036	0.033
	90-130	0.007	0.027	0.029	0.050	0.050

Table 9: Vertical wind shear differences between FUROW & WAsP for a roughness length of 0.1m (green values correspond to positive deviations & blue values correspond to negative deviations).

			Slope (%)				
		Alpha	10.00	20.00	30.00	40.00	50.00
Furow	LWS	10-50	0.076	0.086	0.080	0.032	-0.045
		50-90	0.104	0.088	0.056	0.047	-0.020
		90-130	0.121	0.117	0.094	0.086	0.026
	MWS	10-50	-0.047	-0.033	-0.008	-0.037	-0.057
		50-90	-0.016	-0.015	-0.042	-0.050	-0.090
		90-130	0.012	0.013	-0.012	-0.021	-0.051
	HWS	10-50	0.030	0.048	0.050	0.003	-0.066
		50-90	0.043	0.026	-0.002	-0.016	-0.111
		90-130	0.040	0.037	0.015	0.003	-0.073
WAsP	LWS	10-50	-0.002	-0.004	-0.020	-0.045	-0.126
		50-90	0.096	0.074	0.043	0.010	-0.058
		90-130	0.129	0.095	0.071	0.040	-0.025
	MWS	10-50	-0.123	-0.122	-0.111	-0.115	-0.140
		50-90	-0.023	-0.031	-0.052	-0.083	-0.122
		90-130	0.008	-0.013	-0.038	-0.069	-0.099
	HWS	10-50	-0.047	-0.042	-0.054	-0.076	-0.150
		50-90	0.035	0.008	-0.014	-0.052	-0.144
		90-130	0.033	0.009	-0.014	-0.047	-0.123

Table 10: Vertical wind shear differences between FUROW & OpenFOAM and between WAsP & OpenFOAM for a roughness length of 0.1m (green values correspond to positive deviations & blue values correspond to negative deviations).

- Similar to wind speed-up, WAsP shear tends to deviate from OpenFOAM more for larger slopes, while FUROW tends to deviate more for smaller slopes.
- As expected, differences between the two linear models and OpenFOAM become more marked for lower heights. WAsP has a tendency to underestimate the shear, while FUROW has a tendency to overestimate.
- FUROW and WAsP both tend to overestimate wind shear at lower wind speeds.
- FUROW tends to give shear values that are closer to the OpenFOAM results. The global RMSD with respect to OpenFOAM (calculated for the 45 different cases for each roughness length) is at least 10% closer than for WAsP.

3.4. Results for the horizontal transect

According to the proposed experiment set-up in Fig. 3, reference points have been arranged every 500m except for the hill area where they have been placed every 100m on

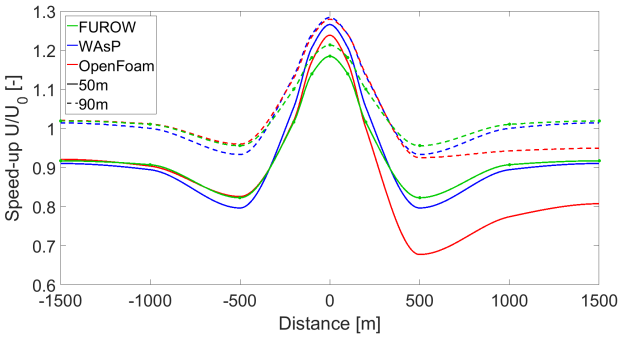

(a) Speed-ups at 50m & 90m

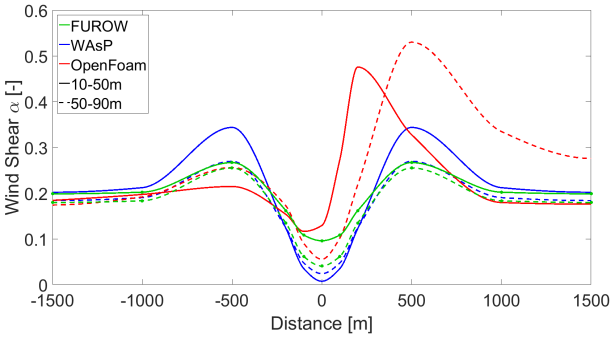

(b) Wind shear in two height ranges

Figure 6: Speed-ups and wind shear for 20% slope, MWS conditions, z_0=0.10m, and for 10-50m & 50-90m

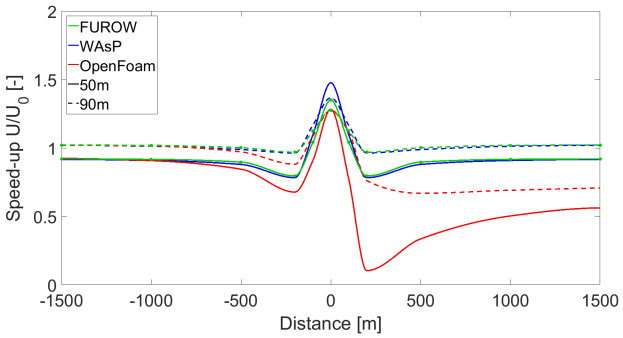

(a) Speed-ups at 50m & 90m

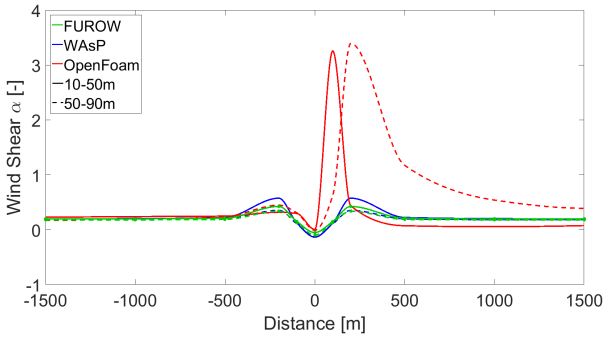

(b) Wind shear in two height ranges

Figure 7: Speed-ups and wind shear for 50% slope, MWS conditions, z_0=0.10m, and for 10-50m & 50-90m

both sides of the hill and up to a distance of 200m from the hilltop. This procedure allows reasonable comparison of wind flow throughout the hill area between FUROW and WAsP. Since comparisons can be very massive due to the high number of experiments, the results of experiments with a 20% and a 50% average slope, MWS conditions and roughness length of 0.10m have been selected as representative. Figs. 6 & 7 show typical speed-up changes. Both models exhibit the same behavior although FUROW seems to produce smoother changes than WAsP, as the latter induces an important decrease of wind speed at the start of the hill, and then accelerates faster up to the hilltop. However, these differences diminish as height increases, being negligible at the top of the planetary boundary layer. When the average slope of the hill increases, differences become higher, especially at the hilltop, although changes as the air approaches the hill are also appreciable. As expected, neither of these linear flow models predicts boundary layer separation as well as potential recirculations on the leeward side of the hill when slopes exceed 30% as is predicted by OpenFOAM. As slope increases, the differences on the leeward side become more noticeable between OpenFOAM and the two linear flow models.

More complete results for the rest of the roughness lengths and wind conditions may be seen in Tables 11a-11b. It is clear that the largest differences between the two models is at the hilltop, with the smallest differences far away from the hilltop. Both models exhibit a clear symmetric behavior. Also as expected, the RMSD is highest at large roughness lengths, corroborating the results in Table 4.

FUROW and WAsP speed-ups are compared to OpenFOAM and presented in Tables 12a-12b and Table 13. The comparisons are presented using the RMSD, which for Tables 12a-12b is calculated as in Eq. 12 and in Table 13 is calculated as:

$$RMS\,D_{fo} = \sqrt{\frac{1}{N_x}\sum_{j=1}^{i=N_r}(D_{j,fo})^2}$$
$$RMS\,D_{wo} = \sqrt{\frac{1}{N_x}\sum_{j=1}^{i=N_r}(D_{j,wo})^2} \quad (16)$$

where N_x is the number of x locations (eleven for -1500, -1000, -500, -200, -100, 0, 100, 200, 500, 1000, and 1500m), $D_{j,fo}$ is the speed-up difference between FUROW and OpenFOAM for x position *j*, and $D_{j,wo}$ is the speed-up difference between WAsP and OpenFOAM for x position *j*.

Additionally, the RMSD between FUROW and WAsP for the vertical wind profiles at each reference point has been calculated and reported in Table 11. According to this table, an increment in the roughness length generates larger differences in the vertical profiles, but differences

		X location (m)										
	Roughness	-1500	-1000	-500	-200	-100	0	100	200	500	1000	1500
LWS	0.03	0.01	0.01	0.03	0.04	0.08	0.09	0.08	0.04	0.03	0.01	0.01
	0.10	0.00	0.01	0.03	0.05	0.08	0.10	0.08	0.05	0.03	0.01	0.00
	0.40	0.01	0.01	0.02	0.05	0.09	0.10	0.09	0.05	0.02	0.01	0.01
MWS	0.03	0.01	0.02	0.05	0.07	0.12	0.15	0.12	0.07	0.05	0.02	0.01
	0.10	0.01	0.02	0.05	0.07	0.13	0.15	0.13	0.07	0.05	0.02	0.01
	0.40	0.01	0.02	0.04	0.09	0.14	0.17	0.14	0.09	0.04	0.02	0.01
HWS	0.03	0.01	0.03	0.06	0.09	0.16	0.20	0.16	0.09	0.06	0.03	0.01
	0.10	0.01	0.03	0.06	0.11	0.18	0.21	0.18	0.11	0.06	0.03	0.01
	0.40	0.02	0.03	0.05	0.14	0.21	0.25	0.21	0.14	0.05	0.03	0.02

(a) Slope = 20%

		X location (m)										
	Roughness	-1500	-1000	-500	-200	-100	0	100	200	500	1000	1500
LWS	0.03	0.01	0.01	0.02	0.02	0.05	0.14	0.05	0.02	0.02	0.01	0.01
	0.10	0.00	0.01	0.02	0.02	0.06	0.14	0.06	0.02	0.02	0.01	0.00
	0.40	0.01	0.01	0.02	0.01	0.07	0.13	0.07	0.01	0.02	0.01	0.01
MWS	0.03	0.00	0.01	0.03	0.03	0.09	0.22	0.09	0.03	0.03	0.01	0.00
	0.10	0.00	0.01	0.03	0.02	0.10	0.22	0.10	0.02	0.03	0.01	0.00
	0.40	0.01	0.01	0.03	0.02	0.12	0.21	0.12	0.02	0.03	0.01	0.01
HWS	0.03	0.00	0.02	0.04	0.04	0.12	0.31	0.12	0.04	0.04	0.02	0.00
	0.10	0.00	0.02	0.04	0.02	0.14	0.31	0.14	0.02	0.04	0.02	0.00
	0.40	0.02	0.02	0.04	0.03	0.19	0.32	0.19	0.03	0.04	0.02	0.02

(b) Slope = 50%

Table 11: Vertical profile RMSD (see Eq. 12) for FUROW with respect to WAsP for different conditions along the horizontal transect (red values correspond to larger deviations while green values correspond to smaller deviations).

are not constant along the whole transect. In fact for moderate slopes, an increase of roughness length reduces the average error of the wind profile just before the start of the hill whereas for steeper hills no clear trends have been found. Finally, there is a relationship between the wind profile RMSD and the reference wind speed, such that, higher wind speeds lead to more similar results on the wind profile than lower wind speeds.

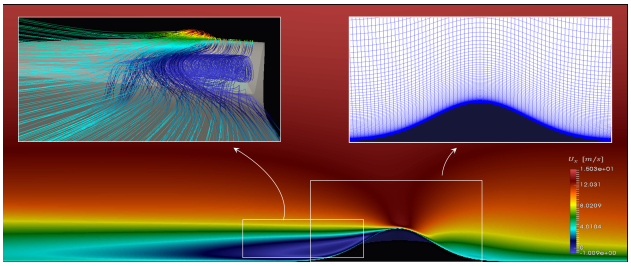

Figure 8: Wind field around 50% slope hill simulated with OpenFoam

The following conclusions can be formulated:

- FUROW gives results closer to OpenFOAM than WAsP for larger slopes. The opposite is true for smaller slopes. FUROW is thus more comparable to the CFD results for complex terrains. This is especially apparent when considering the RMSD, seen in Table 13
- For large slopes, both FUROW and WAsP are far from the OpenFOAM solution behind the hilltop. Recirculations and vortex shedding behind the hill for slopes greater than 30% (see Fig. 8), which are captured by OpenFoam but not by WAsP or FUROW, make the velocity differences larger.

			X location (m)										
		Roughness	-1500	-1000	-500	-200	-100	0	100	200	500	1000	1500
Furow	LWS	0.03	0.04	0.06	0.07	0.10	0.14	0.17	0.14	0.11	0.04	0.03	0.04
		0.10	0.05	0.06	0.08	0.10	0.14	0.17	0.14	0.10	0.03	0.02	0.04
		0.40	0.01	0.01	0.03	0.07	0.11	0.13	0.10	0.10	0.13	0.10	0.07
	MWS	0.03	0.01	0.02	0.01	0.05	0.09	0.12	0.10	0.13	0.22	0.20	0.17
		0.10	0.01	0.01	0.01	0.05	0.09	0.12	0.10	0.13	0.21	0.19	0.17
		0.40	0.07	0.07	0.11	0.09	0.12	0.15	0.13	0.09	0.07	0.08	0.06
	HWS	0.03	0.06	0.07	0.11	0.08	0.13	0.17	0.13	0.09	0.06	0.06	0.03
		0.10	0.10	0.13	0.20	0.14	0.17	0.21	0.18	0.15	0.10	0.06	0.09
		0.40	0.11	0.11	0.18	0.14	0.19	0.23	0.19	0.14	0.07	0.08	0.06
WAsP	LWS	0.03	0.05	0.07	0.10	0.07	0.07	0.08	0.07	0.07	0.06	0.04	0.05
		0.10	0.05	0.07	0.10	0.06	0.06	0.07	0.06	0.06	0.05	0.02	0.04
		0.40	0.02	0.02	0.05	0.02	0.03	0.03	0.05	0.11	0.11	0.09	0.07
	MWS	0.03	0.01	0.02	0.04	0.06	0.06	0.04	0.08	0.15	0.19	0.18	0.17
		0.10	0.01	0.02	0.06	0.06	0.07	0.06	0.09	0.16	0.18	0.17	0.16
		0.40	0.06	0.08	0.14	0.01	0.04	0.03	0.05	0.08	0.06	0.06	0.05
	HWS	0.03	0.07	0.09	0.17	0.01	0.04	0.03	0.04	0.03	0.09	0.04	0.02
		0.10	0.11	0.15	0.25	0.03	0.01	0.01	0.02	0.05	0.16	0.09	0.11
		0.40	0.10	0.12	0.22	0.03	0.06	0.05	0.07	0.08	0.09	0.06	0.04

(a) Slope = 20%

			X location (m)										
		Roughness	-1500	-1000	-500	-200	-100	0	100	200	500	1000	1500
Furow	LWS	0.03	0.02	0.02	0.04	0.10	0.06	0.07	0.23	0.36	0.28	0.20	0.18
		0.10	0.02	0.02	0.04	0.10	0.06	0.07	0.24	0.37	0.30	0.22	0.19
		0.40	0.01	0.01	0.05	0.11	0.09	0.07	0.33	0.48	0.43	0.31	0.27
	MWS	0.03	0.02	0.03	0.10	0.20	0.21	0.11	0.58	0.91	0.80	0.65	0.60
		0.10	0.01	0.03	0.09	0.19	0.21	0.13	0.60	0.92	0.83	0.67	0.61
		0.40	0.05	0.04	0.04	0.12	0.14	0.11	0.45	0.70	0.59	0.47	0.43
	HWS	0.03	0.04	0.04	0.05	0.18	0.22	0.10	0.52	0.90	0.68	0.55	0.51
		0.10	0.05	0.06	0.03	0.17	0.31	0.34	1.36	1.91	1.86	1.19	0.92
		0.40	0.09	0.08	0.06	0.17	0.20	0.16	0.67	1.14	1.01	0.83	0.77
WAsP	LWS	0.03	0.03	0.02	0.03	0.08	0.10	0.07	0.26	0.34	0.26	0.20	0.18
		0.10	0.02	0.02	0.03	0.08	0.11	0.08	0.28	0.36	0.28	0.21	0.19
		0.40	0.01	0.01	0.04	0.11	0.15	0.13	0.38	0.48	0.42	0.31	0.27
	MWS	0.03	0.02	0.03	0.07	0.17	0.29	0.30	0.64	0.88	0.77	0.64	0.60
		0.10	0.01	0.02	0.06	0.17	0.30	0.32	0.67	0.90	0.80	0.66	0.61
		0.40	0.04	0.05	0.03	0.13	0.25	0.26	0.54	0.71	0.57	0.46	0.43
	HWS	0.03	0.05	0.05	0.04	0.15	0.33	0.38	0.60	0.87	0.65	0.53	0.51
		0.10	0.05	0.08	0.04	0.15	0.44	0.63	1.46	1.89	1.81	1.17	0.91
		0.40	0.07	0.08	0.05	0.17	0.37	0.42	0.81	1.16	0.98	0.82	0.78

(b) Slope = 50%

Table 12: Vertical profile RMSD (see Eq. 16) for FUROW & WAsP with respect to OpenFOAM for different conditions along the horizontal transect (red values correspond to larger deviations while green values correspond to smaller deviations).

As for the vertical wind shear, Figs. 6 and 7 show slight differences between the two models for moderate slopes, but as slope increases more noticeable changes are found. WAsP predicts very extreme negative shears even below 100m at the hilltop and large positive shears just before the hill. On the other hand, FUROW wind shear longitudinal distribution is smoother with smaller ranges between maximum and minimum wind shears.

4. Conclusions

With this study it has been shown that FUROW produces similar results to WAsP for simulation of wind flow around hills, but some differences have been found. The FUROW and WAsP models were also compared to a more com-

Wind speed	z_0	FUROW 20%	WAsP 20%	FUROW 50%	WAsP 50%
LWS	0.03	0.085	0.066	0.141	0.142
LWS	0.10	0.084	0.059	0.147	0.151
LWS	0.40	0.079	0.054	0.196	0.210
MWS	0.03	0.101	0.090	0.381	0.401
MWS	0.10	0.098	0.092	0.390	0.411
MWS	0.40	0.094	0.060	0.286	0.316
HWS	0.03	0.092	0.057	0.345	0.377
HWS	0.10	0.140	0.090	0.744	0.786
HWS	0.40	0.137	0.084	0.471	0.519
	Mean	0.101	0.073	0.345	0.368

Table 13: RMSD for speed-up difference for 20% & 50% slope of FUROW and WAsP compared to OpenFOAM.

plex OpenFOAM model, which simulated the wind flow solving the Navier-Stokes equations with a k-ϵ turbulence closure model. The results were coherent with theory and differed most from the linearized flow models on the leeward side of the Gaussian hills, where the symmetric solution given by the linearized theory differs most from asymmetric, non-linear results. FUROW was shown to produce results in complex terrains closer to OpenFOAM than WAsP. Nonetheless, it would be necessary to compare with on-site measurements to ensure the veracity of the results. It would also be recommendable to test different turbulence closure models in OpenFOAM to explore model sensitivity.

The main conclusions extracted from the study are the following:

- Wind speed distribution in both models agrees well along the whole horizontal hill transect. Differences in the vertical profile between FUROW and WAsP increase with the hill slope.
- Maximum discrepancies between the FUROW and WAsP models in the vertical profile are found at the hilltop.
- Besides for high roughness lengths, wind shear calculated for three hub height ranges agrees well between models, but changes along the hill are more significant in the WAsP model than in FUROW, which exhibits a smoother behavior.
- Higher roughness length induces larger differences on the vertical profile at lower levels.
- Differences between models diminish as wind speed magnitude increases, as higher wind speeds are more typical of purely neutral conditions for which linearized models should perform better.
- FUROW is appropriate for calculation of wind flow over complex terrain, as it is comparable to the results provided by a CFD software, but at a much shorter computational time. Consequently, FUROW can be considered a suitable software to estimate correctly the wind resource and thus improve the energy production predictions.

References

[1] Jackson, P.S. and Hunt, J.C.R. (1975), "Turbulent wind flow over a low hill", J. Royal Met. Soc. 101, pp 929-955.

[2] Troen, I. (1990) A high resolution spectral model for flow in complex terrain. Ninth Symposium on Turbulence and Diffusion. American Meteorological Soc., Riso National laboratory, Denmark, 417-420.

[3] "Wind energy industry-standard software - WAsP. DTU Wind Energy, http://www.wasp.dk/. 28 August 2016."

[4] Beaucage P. and Brower M.C. (2012), "Do more sophisticated models produce more accurate wind resource estimates?", Wind Flow Modeling Performance, Publication by AWS Truepower.

[5] Mortensen N.G., Bowen A.J. and Antoniou I. (2006), "Improving WAsP predictions in (too) complex terrain", Publication at EWEC 2006.

[6] Troen, I. and Petersen, E.L (1989). European Wind Atlas. Published by Riso National Laboratory, Roskilde, Denmark, ISBN 87-550-1482-8.

[7] Giebel, G. and Gryning, S.E. (2007) Shear and stability in high met masts and how WAsP treats it. Published by Riso National Laboratory, Roskilde, Denmark

[8] Crespo, A., Migoya, E., García, J., Manuel, F., Prieto, J.L. (2010) Efectos topográficos en el recurso eólico. Solar Decathlon Europe 2010. Madrid, España, 17-27 junio, 2010.

[9] Migoya, E., Crespo, A., Jiménez, A., García, J., Manuel, F. (2007). Wind energy resource assessment in Madrid Region. Renewable Energy, Nº 32, pp 1467-1483.

[10] Belcher, S.E. and Hunt, J.C.R. (1998), "Turbulent flow over hills and waves", Annu. Rev. Fluid Mechanics 30, pp 507-538.

[11] Gryning, S.E., Batchvarova, E., Brümer, B., Jorgensen, H. and Larsen, S. (2007), "On the extension of the wind profile over homogeneous terrain beyond the surface boundary layer" Boundary-Layer Meteorology, Volume 124, Issue 2, pp 251-268.

[12] Garratt, J.R. (1994), "The atmospheric boundary layer", Cambridge Atmospheric and Space Science Series.

[13] Dyer, A.J. (1974), "A review of flux-profile relationships", Boundary-Layer Meteorology, Volume 7, Issue 3, pp 363-372.

[14] Yagüe, C., Viana, S., Maqueda, G. and Redondo, J.M. (2006), "Influence of stability on the flux-profile relationships for wind speed φm and temperature φh for the stable atmospheric boundary layer", Nonlinear Processes in Geophysics, 13, pp 185-203.

[15] Inoue, E. (1963), "On the turbulent structure of airflow within crop canopies", Journal of the Meteorological Society of Japan, Section II, 41, pp 317-326.

[16] SOLUTE Ingenieros (2016), "FUROW Theory manual v1.1"

[17] "OpenFOAM: The open source CFD toolbox. ESI Group, www.openfoam.com. 22 August 2016."

[18] Krüger O., Schrödinger C., Lengwinat A., Paschereit C. O. "Numerical modeling and validation of the wind flow over the Lake Wannsee", WCCM XI, July 20-25, 2014.

[19] Launder B.E., and Spalding D.B. (1972), Lectures in Mathematical Models of Turbulence, Academic Press, London.